High purity H_2 by sorption-enhanced chemical looping reforming of waste cooking oil in a packed bed reactor

P. Pimenidou[1], G. Rickett[1], V. Dupont[1]*, M. V. Twigg[2]

[1]*Energy and Resources Research Institute, SPEME, The University of Leeds, Leeds LS2 9JT, UK*

[2]*Johnson Matthey Plc, Orchard Laboratory, Orchard Road, Royston, SG8 5HE, UK*

Corresponding author: V.Dupont@leeds.ac.uk

Paper accepted and published. Full reference:

Pimenidou, P., Rickett, G. L., Dupont, V, Twigg, M. V. 2010. High purity hydrogen by sorption enhanced chemical looping reforming of waste cooking oil in a packed bed reactor. Bioresource Technology 101 (2010) 9279–9286.

Abstract

High purity hydrogen (>95%) was produced at 600 °C and 1 atm by steam reforming of waste cooking oil at a molar steam to carbon ratio of 4 using chemical looping, a process that features redox cycles of a Ni catalyst with the in-situ carbonation / calcination of a CO_2-sorbent (dolomite) in a packed bed reactor under alternated feedstreams of fuel-steam and air. The fuel and steam conversion were higher with the sorbent present than without it. Initially, the dolomite carbonation was very efficient (100 %), and 98 % purity hydrogen was produced, but the carbonation decreased to around 56% with a purity of 95% respectively in the following cycles. Reduction of the nickel catalyst occurred alongside steam reforming, water gas shift and carbonation, with H_2 produced continuously under fuel-steam feeds. Catalyst and CO_2-sorbent regeneration was observed, and long periods of autothermal operation within each cycle were demonstrated.

Keywords: chemical looping; reforming; in-situ sorption; waste oil; nickel; dolomite.

Introduction

The process of chemical looping has been the focus of growing attention in the past decade as a means of large scale power generation minimising CO_2 emissions, by either producing a sequestration-ready CO_2 effluent (chemical looping combustion) or decarbonising the fuel (chemical looping reforming). The production of hydrogen of high purity using process intensification measures such as chemical looping is desirable in chemical plants and petroleum refineries, as well as upstream of a fuel cell to alleviate the energy burden placed on gas separation and purification. Suitable feedstocks for steam reforming and steam gasification can be found in many commercial and industrial waste streams of biomass origins. These would typically have significant moisture content, such as the crude glycerol by-product of the transesterification of vegetable oils (Dou et al, 2009), and other $2^{nd}/3^{rd}$ generation biofuels such as biomass pyrolysis oils, or micro algae suspensions. Used vegetable cooking oils exhibit a higher free fatty acid content, viscosity and polarity than the virgin oils, which makes their conversion to the fatty acid methyl esters of the biodiesel blend difficult. In the present study, waste cooking vegetable oil is converted to a nearly pure hydrogen gas separate from the CO_2 waste stream, using an advanced steam reforming process. The latter combines the chemical looping of a Ni-based catalyst as oxygen transfer material (OTM) and of a natural CO_2 sorbent (dolomite), in a packed bed reactor. It has been shown in a previous publication that the Ni in the catalyst could repeatedly reduce and oxidise during the chemical looping reforming of waste cooking vegetable oil (WCO) in the absence of a CO_2 sorbent (Pimenidou et al, in press). The present work focuses on the ability of the CO_2 sorbent to repeatedly carbonate while generating a pure H_2 gas under the fuel/steam feed, and to regenerate to its calcined oxide form under the air feed during the chemical looping reforming of the same waste oil. The aim of this study was to

carry out a number of cycles with high H_2 purity syngas production while attempting to operate as close to autothermal as possible, that is, with little or any heat being supplied to the reactor.

2 Materials and Methods

2.1 Materials

The OTM catalyst consisted of 18 wt % NiO supported on Al_2O_3 from Johnson Matthey, originally supplied in pellet form, broken up and sieved to 0.85-2 mm size particles. The CO_2 sorbent was pre-calcined dolomite from the Warmsworth quarry (South Yorkshire, England) broken up and sieved to the same size as the catalyst. 40g of fresh catalyst, with or without intimate mixing with 40 g of the calcined CO_2 sorbent, were loaded at the centre of the reactor, preceded by 25 mm thick plug of spherical Al_2O_3 beads. The as-received dolomite was fully carbonated and had a composition of 21.3 wt% MgO, 30.7 wt% CaO, 0.3 wt% SiO_2, 0.27 wt% Fe_2O_3, and 0.1 wt% Al_2O_3, and 47.33 wt% CO_2.

The waste cooking vegetable oil (WCO) contained 74.9 wt% C, 12.85 wt% H, 12.15 wt% O and 0.10 wt% N, had a liquid density of 920 kg m^{-3} at 20 °C and a gross calorific value of 39.5 MJ kg^{-1}. Based on its elemental mass formula, its average elemental molar formula was $C_1H_{2.04}O_{0.122}$. Details of the analytical techniques used for the oil characterisation can be found in Pimenidou et al, 2010. The molar formula was equivalent to $3(CH_{1.67} + C_{18}H_{37.1}O_{2.31})$, where '$CH_{1.67}$' represents the portion of non-oxygenated glycerol 'backbone' molecule per fatty acid chain, and where the 'C_{18}' fatty acid chain is chosen here to reflect on the WCO's origin as rapeseed oil. The oxygen content of 2.31, larger than the expected 2 of vegetable fatty acid chains, confirmed the increased polarity of the waste oil compared to that of its virgin rapeseed oil source.

2.2 *Reactor set-up and experimental procedure*

A detailed description of the reactor set up, including a diagram, is given in Pimenidou et al (2010). To summarise, a stainless steel temperature controlled and kaowool insulated reactor of ID 2.05 cm and 26.9 cm length, providing 89 cm^3 volume containing the bed materials (40 g of 18wt%NiO/Al_2O_3 catalyst with or without 40 g calcined dolomite), was fed from the bottom via a co-axial injector with steam in the inner pipe, preheated to 150 °C and near-vapourised WCO in the annular space at 300 °C. When not using the CO_2-sorbent, the experiments were carried out both manually diluted with Al_2O_3 beads (D_{beads} ≈1.5 mm) to achieve the same reactor bed volume as when using the sorbent, and undiluted, thereby achieving roughly half the bed volume than when using the CO_2 sorbent. As the observed reactant conversions were very poor and accompanied by excessive carbon deposition when using the Al_2O_3 beads dilution, subsequent experiments were carried out without it. Peristaltic pumps maintained the liquid flows of WCO and water at 0.55 and 2.32 $cm^3\ min^{-1}$ (20 °C) respectively, achieving a molar steam to carbon ratio of 4. The steam to carbon ratio of 4 provided a better operation than 2.5 in the absence of CO_2 sorbent (Pimenidou et al, 2010) and thus was chosen for the present study. A gas flow of 600 $cm^3\ min^{-1}$ (STP) of N_2 was employed during the fuel/steam feed and the N_2 purge period separating the fuel/steam feed from the air feed, as in the chemical looping experiments without sorbent reported in Pimenidou et al (2010). The air flow rate was also 2000 $cm^3\ min^{-1}$ (STP) during the air feed. The reactor effluent passed through two condensers and water traps prior to online analysis every 5 seconds of CO, CO_2 and CH_4 by non-dispersive infra-red absorption, H_2 by thermal conductivity detection and O_2 via paramagnetic analysis, using Uras 14, Caldos 15 and Magnos 106 ABB analysers respectively. It was shown through off-line GC-FID analysis that there were no other higher hydrocarbons produced in the same set up without sorbent

(Pimenidou et al, 2010), and therefore the dry gases were also assumed here to contain N_2 molar fractions corresponding to the balance to 1 of the sum of the CO, CO_2, CH_4, H_2 and O_2 measured mol fractions.

The procedure followed to pre-reduce the catalyst to initiate the cycling experiments is described in detail in Pimenidou et al, 2010. In the present work, the reactor temperature was set at 600 °C for all the experiments under both fuel-steam and air feeds. Three thermocouples placed in the middle of the reactor bed, above and below the middle, measured the temperatures at 1 second intervals, allowing the monitoring of the endotherms and exotherms resulting from the reactions during both feeds.

2.3 *Reactions and output calculations*

The reaction mechanism under each type of feed is outlined in the first two sub-sections, followed by the energetic of the process under the two feeds and a description of the equations used to derive the process outputs. A nomenclature is provided in the appendix.

2.3.1 Reaction mechanism under fuel/steam/N_2 feed (reducing mode):

An oxygenated hydrocarbon fuel with a molar elemental formula of $C_nH_mO_k$, reduces the oxidised catalyst via the unmixed combustion reaction henceforth termed 'UC' (Dupont et al, 2007), producing CO_2 and H_2O as by-products. While NiO undergoes reduction, significant coking may occur from the thermal decomposition of the fuel and of its pyrolysis products. The maximum reduction rate of NiO is therefore $(2n+0.5m-k)$ mol per mol of $C_nH_mO_k$ fuel converted. This emphasises the relative positive contributions of both the C and H fuel-contents to the NiO reduction rate, in contrast to the negative contribution of the O fuel-content. Once Ni is sufficiently reduced, steam reforming of the WCO, henceforth termed 'SR' can occur on the catalyst, with CO and H_2 as the products, which is followed by in-situ water gas shift 'WGS'.

Both the UC and SR/WGS reactions are then followed by the carbonation ('Carb') of the calcined sorbent. When using dolomite as the sorbent, this is a chemisorption reaction, where only Ca, and not Mg, acts as the active site for the carbonation.

According to Le Chatelier's principle, by shifting the equilibria the CO_2-producing reactions UC and WGS to the right, the carbonation of the Ca-based sorbent allows not only the elimination of CO_2 from the gases, promoting UC, but also a decrease in the amount of CO produced, thereby further promoting SR. This results in an increased fuel conversion, a process termed 'sorption enhancement'. Once SR and WGS are established, a nearly pure H_2 gas evolves, eliminating the need for the downstream high- and low- temperature water gas shift reactors required by a conventional steam reforming process. Thus sorption enhancement represents a process intensification measure. The production of the by-products methane and carbonaceous deposits during this feed would be accompanied by a lower H_2 yield, here defined by the molar ratio of H_2 produced to the theoretical maximum mol of H_2 from the complete SR and WGS reactions. Assuming complete reactions SR and WGS in the absence of UC, and notwithstanding thermodynamic limitations (mainly due to reverse-WGS), the maximum hydrogen purity can be calculated as:

H_2 max purity = $100 \times \dfrac{(n+m/2-k)+n}{n+n+(n+m/2-k)} = 74.3\%$ for the WCO.

With a carbonation reaction achieving complete removal of CO_2, and ignoring thermodynamic limitations, the maximum H_2 purity becomes 100 %. The maximum production of H_2 obtainable from sorption enhanced steam reforming the WCO, again disregarding thermodynamic limitations, is therefore 2.90 mol H_2 /mol of C in the fuel-feed.

2.3.2 Reaction mechanism under air feed (oxidising mode)

Upon switching to air feed, the carbon deposits burn via full or partial oxidation ('C-Ox' and 'C-POx') depending on the reactor bed temperature, magnitude of the air flow and the oxidation reactions being or not mass transfer limited. The Ni on the catalyst support then consumes oxygen via Ni oxidation to NiO ('Ni-Ox').

In the presence of a carbonated sorbent, the higher temperatures reached during the air feed allow the sorbent to regenerate through decarbonation, also called calcination, henceforth termed 'Calc'.

2.3.3 Energetics under the two feeds

In the described mechanism, the UC, SR and Calc reactions are endothermic, while WGS, Carb, C-Ox, C-POx, and Ni-Ox exothermic. Of the latter, C-Ox and C-POx are more likely to occur on the outer surface of the reactor bed particles, where carbon filaments may form, where they generate a heat that may be easily swept away by the gas flows. In contrast, the Ni-Ox and Carb reactions are highly exothermic reactions which take place deeper within the particles of catalyst and sorbent respectively. Despite the ability of the sorption enhanced chemical looping reforming process to cope with coking fuels by cyclically oxidising the carbon deposits (unlike conventional catalytic steam reforming), it remains desirable to prevent coke deposition from the point of view of both optimising heat transfer and achieving a maximum H_2 yield. Without carbon deposition, the heat transfer would be expected to move deeper in the reactor bed and allow better coupling of the oxidation of nickel with the strongly endothermic calcination (regeneration) of the sorbent.

2.3.4. Calculation of process outputs

While carbonation occurred, the output gas did not contain CO_2, and we shall see in the results section, that CO and CH_4 concentrations were also negligible. With more time on stream, the sorbent began to saturate, corresponding to a CO_2-breakthrough period. Finally, the sorbent reached its maximum sorption capacity for the conditions of the experiment, and a 'CO_2-steady state' was established, similarly to the one that occurred in the absence of sorbent (Pimenidou et al, 2010). We are mindful of not calling this regime a full steady-state as transient reactions involving NiO reduction or carbon deposition may still be occurring.

- Fuel conversion fraction during the fuel/steam/N_2 feed:

Direct calculations of the fuel conversion during CO_2 sorption via the carbon balance were not possible due to the inability to measure the carbonation rate '$\dot{n}_{CO2,carb}$' on the solid sorbent at any given time prior to, or during CO_2 breakthrough. However, assuming the expected effect of sorption enhancement, caused by the coupling of UC with Carb, or (SR+WGS) with Carb, a minimum fuel conversion fraction '$X_{WCO,PB}$' during carbonation prior to- and during CO_2-breakthrough could be estimated by approximating it to the conversion reached at the CO_2-steady state (post-CO_2 breakthrough):

$$X_{WCO,PB} \approx X_{WCO,BT} \approx X_{WCO,SS} = \frac{\dot{n}_{WCO,in} - \dot{n}_{WCO,out}}{\dot{n}_{WCO,in}} = \frac{\frac{\dot{n}_{N_2,in}}{y_{N_2,SS}}\left(y_{CH_4} + y_{CO} + y_{CO_2}\right)_{ss}}{n \times \dot{n}_{WCO,in}} \quad \text{Eq.1}$$

Where the suffix '*PB*' stands for 'prior to CO_2 breakthrough or pre-CO_2 breakthrough', '*BT*' means 'during CO_2-breakthrough', and '*SS*' is 'at CO_2-steady state, post CO_2-breakthrough'. In Eq. 1 and the following equations, the $\dot{n}$ symbol is used to represent a molar rate, and *y*, a mol fraction, while the constants *n*, *m* and *k* represent the elemental molar composition of the WCO fuel ($C_nH_mO_k$).

- Sorbent carbonation rate and total carbonation efficiency during the fuel/steam/N_2 feed:

Using the value of $X_{WCO,PB}$ derived with Eq. 1, as well as the knowledge of the molar production rates of the carbon containing co-products CO and CH_4, an estimate of the total molar production rate of CO_2 and thus of carbonation rate ($\dot{n}_{CO_2,carb}$) could be obtained via Eq. 2 below:

$$\dot{n}_{CO_2,carb} = nX_{WCO,PB,BT}\dot{n}_{WCO,in} - \left(\frac{\dot{n}_{N_2,in}}{y_{N_2,PB,BT}}\right)\left(y_{CO} + y_{CH_4} + y_{CO_2}\right)_{PB,BT} \quad \text{Eq. 2}$$

In the RHS of Eq. 2, the first, positive term represents the molar rate of carbon converted from the fuel, and the second, negative term, the molar evolution rates of the gaseous carbon-containing products.

Prior to CO_2-breakthrough, since none of the carbon containing products were detected, as will be seen in the results section, the negative term in Eq. 2 was negligible, and $\dot{n}_{CO_2,carb}$ was able to simplify to the first positive term only. During CO_2-breakthrough, the second negative term was significant and accounted for the simultaneous emergence of CO_2, CO and CH_4 in the output gas stream.

Equation 3 gives the total carbonation efficiency as the sum of the carbonation efficiencies prior to and after CO_2 breakthrough, obtained by integration of the carbonation rates over the characteristic durations of pre-CO_2 breakthrough and CO_2 breakthrough regimes.

$$\alpha = \alpha_{PB} + \alpha_{BT} = 100 \times \frac{\left(nX_{WCO,PB}\dot{n}_{WCO,in} \times \left(t_{BT} - t_0\right)\right) + \int_{t_{BT}}^{t_{SS}} \dot{n}_{CO_2,carb,BT}\, dt}{n_{CO_2,\max}} \quad \text{Eq.3}$$

In Eq. 3, t_0 is defined as the time at breakthrough of H_2 , taken as evidence of onset of sorption enhanced steam reforming, t_{BT} was the time at breakthrough of CO_2, when the sorbent began to reach its capacity, and t_{SS}, was the time at reaching CO_2 steady state, evidencing the sorbent having reached its maximum capacity.

It was of interest to split the total carbonation efficiency 'α' during fuel and steam feed into its pre-breakthrough (α_{PB}) and breakthrough contributions (α_{BT}) because for the former, H_2 purity was close to 100%, while for the latter, the H_2 purity slowly decreased to the steady state of the non-sorption enhanced process (ca. 70%). For some applications such as proton exchange membrane fuel cells (PEMFC), which are very sensitive to H_2 purity, maximising the duration of the pre-CO_2 breakthrough period is desirable, whereas for solid oxide fuel cells (SOFC) or molten carbonate fuel cells (MCFC), more tolerant of other syngas compounds, H_2 purity may not be so critical.

The carbonation efficiency values were calculated for each performed cycle to assess the sorbent performance over repeated sorption enhanced chemical looping reforming cycles of the waste cooking oil.

- Steam conversion fraction during the fuel/steam/N_2 feed:

In the steam reforming coupled with water gas shift, the production of hydrogen is the result of the contributions of the fuel-hydrogen and of the steam-hydrogen. Generally, for a '$C_nH_mO_k$' oxygenated fuel reacting with ($2n$-k) H_2O via SR/WGS, the maximum production of H_2 is (($2n$-k)+0.5m), indicating clearly that in conditions of maximum H_2 production, the steam contribution fraction is ($2n$-k)/($2n$-k+0.5m) and that of the fuel, 0.5m/($2n$-k+0.5m). For the $C_1H_{2.04}O_{0.122}$ waste cooking oil, the steam contribution can therefore account for 64.9% of the H_2 produced through SR/WGS, while that of the fuel is only 35.1%. Therefore steam conversions, which are rarely reported in the literature on steam reforming, have a great effect on the material efficiency of the process. Factors limiting the steam conversion are not only equilibrium limitations, which the presence of the CO_2-sorbent intend to overcome, but also the catalyst's activity in both the steam reforming and the water gas shift reactions.

Using the fuel conversion fraction from Eq.2 and an elemental balance on hydrogen, a minimum value for the steam conversion fraction can be estimated using Eq. 4 below:

$$X_{H_2O,PB} \approx X_{H_2O,BT} \approx X_{H_2O,SS} = \frac{1}{2\dot{n}_{H_2O,in}} \times \left[\frac{\dot{n}_{N_2,in}}{y_{N_2,SS}} \left(4y_{CH_4} + 2y_{H_2} \right)_{SS} - m\left(\dot{n}_{WCO,in} X_{WCO,SS} \right) \right] \quad \text{Eq. 4}$$

The first, positive term in the RHS of Eq. 4 represents the formation of the hydrogen containing products and the second, negative term accounts for the known contribution of the fuel to the hydrogen products, leaving only the contribution of water to the same.

- Selectivity of the carbon-containing products in the gas phase during the fuel-steam feed:

These were defined as:

$$Sel_{\mathrm{CH_4\ or\ CO\ or\ CO_2}}(\%) = 100 \times \frac{y_{\mathrm{CH_4\ or\ CO\ or\ CO_2}}}{y_{CH_4} + y_{CO} + y_{CO_2}} \quad \text{Eq.5}$$

- NiO molar reduction rate and extent of NiO reduction during fuel-steam feed:

From an elemental balance of oxygen, it is possible to also estimate a constant rate of NiO reduction during carbonation, and thus establish whether reduction of the catalyst (UC) may have been concurrent with steam reforming (SR) and carbonation (Carb). This is expressed in Eq. 6:

$$\dot{n}_{NiO \rightarrow Ni,PB} = \dot{n}_{out,dry,PB} \left(y_{CO} + 2y_{CO_2} \right)_{PB} + 2\dot{n}_{CO2,carb} - \left(\dot{n}_{H2O,in} X_{H2O,PB} \right) - k\left(\dot{n}_{WCO,in} X_{WCO,PB} \right) \quad \text{Eq.6}$$

Where the values of $X_{WCO,\,PB}$, $\dot{n}_{CO_2,carb}$ and $X_{H2O,PB}$, were pre-determined by Eqs. 1, 2 and 4.

In the RHS of Eq. 6, the first, positive term represents the molar rate of O leaving the reactor as gaseous products (no O_2 is produced under these reducing conditions), the second positive term is the molar rate of O creating the carbonate, and the last two negative terms represent the molar rate of O converted from water and fuel respectively.

However, in the pre-breakthrough regime, where H_2 was the only dry gas product detected, Eq. 6 was able to simplify to Eq. 7 below:

$$\dot{n}_{NiO\rightarrow Ni,PB} = \dot{n}_{WCO,in} X_{WCO,SS}\left(2n + 0.5m - k\right) - y_{H_{2,SS}} \frac{\dot{n}_{N_2,in}}{\left(1 - y_{H_2,SS}\right)} \quad \text{Eq. 7}$$

The equation above reflected that the NiO reduction rate prior to CO_2 breakthrough, i.e. when H_2 was the only gas product, was equal to the maximum rate of reduction arising from fuel conversion ($\dot{n}_{WCO,in} X_{WCO,SS}\left(2n + 0.5m - k\right)$) through the unmixed combustion reaction, minus the molar rate of hydrogen evolving from the process. This is because one mol of H_2 could potentially have reduced an additional mol of NiO to Ni by forming water. It has to be stressed that Eq. 7 is not expected to provide an accurate value of the reduction rate of NiO at any given time prior to CO_2 breakthrough, but is a time-averaged estimate, as any transient effect that the rate may have undergone, e.g. early peak followed by drop, would not be accounted for. The purpose of this equation was to merely help assess whether the NiO reduction via unmixed combustion was more likely to have occurred prior to, or concurrently to steam reforming, its fuel-consuming competitor, where the latter situation may be preferable due to allowing H_2 production earlier in the process.

3. Results and discussion

3.1 *Process outputs during WCO/steam/N_2 feed*

3.1.1 Steam reforming outputs and energetics

H_2 and CO_2 mol fractions measured during the WCO/steam/N_2 feeds for 6 cycles conducted in the presence of the CO_2-sorbent dolomite are shown in Fig.1(a), with Fig. 1(b) showing the electrical power input to the reformer in % of the maximum.

There was a long period in Fig. 1b where the power input to the reformer was automatically cut off, corresponding to a visible lack of CO_2 in the products in Fig. 1a, as the heat produced in the reactor from the carbonation reaction caused the temperature to exceed the set point of 600 °C. In the case of the first cycle, this period lasted 700 seconds. This illustrated the increased energy efficiency of the sorption enhanced chemical looping reforming process over that of the conventional steam reforming process.

The H_2 % purity, defined here as the % dry mol fraction ratio of H_2 to the sum of the H_2, CO, CO_2 and CH_4, i.e. the H_2 mol % corrected for 0 N_2, is plotted with time on stream for the six cycles in Fig. 2, focusing mainly on the pre-CO_2 breakthrough period. Figures 1a and 2 indicated that all the cycles exhibited a period of time where the only significant gas species in the reactor products was hydrogen, these corresponded to purities above 90% between 800 and 1400 s for all the cycles, and 97% purity reached for cycles 1 and 6 for more than 700 s. Therefore, as expected from sorption enhancement, during this period the effect of the sorbent was to, not only fully chemisorb CO_2, but also to cause nearly complete conversion of CO and CH_4, virtually eliminating them from the syngas. The following section assesses the efficiency of the process via the fuel and steam conversion fractions, selectivity of the carbon containing products, and H_2 purity in post CO_2-breakthrough conditions (steady state 'SS'), listed in Table 1. Note that the H_2 purity listed in table 1 are the minimum values reached in Fig. 2 after the plateaus of high purity

of pre-CO_2 breakthrough. These outputs are compared to the corresponding process for the same conditions in the absence of CO_2 sorbent in the reactor (results of the study published in Pimenidou et al, 2010). We have shown in Pimenidou et al (2010), that when operating with a mass of 80 g of the NiO-Al_2O_3 catalyst at the same feed flows as the present work, WCO conversion fractions of average 0.9 and steam conversion fractions of 0.27 were recorded over 6 cycles. This contrasted with the results when using only 40 g of catalyst with the same feed rates, which only achieved WCO and steam conversion fractions of 0.2 and 0.06 respectively, also averaged over 6 cycles. Unfortunately the size of the reactor meant that more than 80 g of bed material could not be accommodated in the reactor. Therefore the present conditions of 40 g catalyst with 40 g calcined dolomite using the same feed rates were not expected to yield WCO and steam fractions exceeding 0.20 and 0.06 by significant amounts. Surprisingly, a comparison of the two conditions '40 g of catalyst' vs. '40 g catalyst + 40 g dolomite' in Table 1 shows that the WCO and steam conversion fractions post-CO_2 breakthrough were significantly larger in the presence of the sorbent for the 6 cycles than without the sorbent, with average values of 0.31 and 0.12 respectively. This may have been caused by the catalytic cracking activity of dolomite, and its resistance to coking, as previously observed by Simell and Son-Bredenberg (1990), Myren et al (2002), Devi et al (2005) and Srinakruang et al (2006). The first cycle with the sorbent exhibited the highest reactant conversions, with WCO and steam conversion fractions of 0.46 and 0.19. From the 2^{nd} cycle, the process outputs lowered to nearer the average and, notwithstanding a dip during the 5^{th} cycle, remained around the average for the remainder of the

cycles. The highest conversions observed in the first cycle were accompanied by a mid-reactor temperature lower than the average by 15 °C, reflecting the endothermicity of SR in post-CO_2 breakthrough conditions. The lower temperature in turn affected the selectivity of the carbon containing products, with higher CH_4 and lower CO. As the cycles settled into a less performant fuel conversion, the heat demand in the reactor decreased accordingly and the mid reactor temperature remained close to the set temperature of 600 °C.

The H_2 purity during CO_2-steady state (post-CO_2 breakthrough) was, with an average of 70.7 %, close to the theoretical maximum in absence of carbonation of 74.3% and notwithstanding thermodynamic limitations quoted in section 2.3.1. A more realistic comparison can be made by using thermodynamic equilibrium calculations following the methodology outlined in Pimenidou et al (2010), and previously applied to the reactor without sorbent, using the mid-reactor temperature as input and assuming the typical rapeseed oil composition used in Pimenidou et al (2010). This new calculation yielded H_2 purities between 69.4 % and 70.2%, with an average of 70.0% over the 6 cycles, in very good agreement with the measurements. The selectivity to CO, CO_2 and CH_4 products with time-on-stream in post-CO_2 breakthrough conditions is listed in Table 1. The high selectivity to CO_2 between 78% and 89% indicated there must have been good conditions for sorption enhancement of the chemical looping reforming during the preceding carbonation period. The values predicted by the equilibrium calculations were $Sel_{CO,\,eq}$=21-25%, $Sel_{CO2,eq}$ =70%, $Sel_{CH4,eq}$=5-8%, which would have been less propitious for CO_2 sorption. This calculated equilibrium selectivity was however reproduced quite closely by the experiments without CO_2 sorbent in the reactor, as can be seen in Table 1.

3.1.2 Carbonation efficiency

Using the mass of calcined dolomite present in the reactor (40 g) and the known mass fraction of CaO in the fully carbonated sorbent (0.307), the maximum molar capacity for CO_2 capture $n_{CO_2,\max}$ was calculated to be 0.417 mol. The characteristic times t_0, t_{BT} and t_{SS} are indicated in Fig.1 for the first cycle, representative of all the cycles. Table 2 lists the values of (t_{BT} - t_0), (t_{SS} - t_{BT}), i.e. the durations prior to- and during CO_2-breakthrough, and their carbonation efficiencies α_{PB}, α_{BT}, with the total α, for the six cycles carried out with the sorbent in the reactor using Eq. 3. Given the error-propagating nature of the calculation of the total carbonation efficiency α via Eq. 3, it was remarkable that the obtained value for the first cycle, at 101%, was so near 100%. It was also expected from previous dolomite carbonation studies (Pimenidou et al, 2009), that the first cycle be able to fully carbonate the sorbent, as was the case here. The values in table 3 indicate that α decreased sharply in the second cycle, but more or less stabilised for the remainder of the cycles to an average of 55.9 % over cycles from 2 to 6. Decreases of carbonation efficiency upon repeated cycling were expected for calcined dolomite, which, as all un-pretreated natural CaO-based sorbents, would have exhibited poor chemical stability due to sintering (Harrison, 2008).

With regards to the pre-CO_2 breakthrough carbonation efficiency α_{PB}, it exhibited the same trend as α, with a maximum obtained in the initial cycle (74 %) followed by a sharp decline and stabilisation at around 42 % to the exception of cycle 5. In the observed absence of carbon containing products during pre-CO_2 breakthrough, there were two main parameters that contributed to the value of the pre-CO_2 breakthrough carbonation efficiency α_{PB} : the WCO fractional conversion X_{WCO}, which determined the rate of CO_2 production and thus controlled that of carbonation, and the pre-CO_2 breakthrough duration (t_{BT} - t_0), over which the rate of

carbonation was integrated. Table 2 indicates that the low value of α_{PB} obtained in cycle 5 (17.3%) was not due to (t_{BT} - t_0), which itself was of similar duration as cycles 3 and 4, but to the lower fraction of fuel conversion (0.23), the lowest of the 6 cycles. This suggests not a limitation of the carbonation process but a momentary abnormality in the activity of reactions UC, SR and WGS. Accordingly, this low pre-CO_2 breakthrough carbonation efficiency was later compensated by a longer CO_2-breakthrough period, yielding a total efficiency close to those of the post-initial cycles. It is difficult to find a reason for the lower WCO conversion obtained at cycle 5, as the experiments without sorbent did not exhibit this anomalous dip in conversion, and the cyclic experiments were carried out without interruption.

Sustaining the relatively high level of carbonation for six cycles is a strong indicator that regeneration of the sorbent must have occurred to a significant extent via the exotherms generated during the air feed steps introduced between each WCO/steam/N_2 feeds, which will be verified qualitatively in the 'air feed' section of the results.

3.1.3 NiO reduction

Table 3 lists the pre-CO_2 breakthrough values of the NiO reduction rate $\dot{n}_{NiO\rightarrow Ni,PB}$ per cycle using Eq. 7, derived from the elemental balance of oxygen, alongside the fuel conversion fraction. One would expect the two parameters to follow the same trend since the H_2 mol fraction reached at CO_2-steady state, $y_{H2,SS}$, varied little over the six cycles, and the remaining terms in Eq. 7 were input values that remained constant for all the cycles. Nevertheless, the term $y_{H_{2,SS}} \frac{1}{\left(1-y_{H_2,SS}\right)}$ in Eq. 7 exacerbated the small variations in $y_{H2,SS}$ and was responsible for the slight divergence between them. Using Eq. 7, and integrating the estimated NiO reduction rate during pre-CO_2 breakthrough until 100% of the NiO was reduced, yielding the number of Ni

moles produced (Δn_{Ni}), a 'time to final reduction' (t_{FR}) could be obtained, where $t_{FR} = \dfrac{\Delta n_{Ni}}{\dot{n}_{NiO \rightarrow Ni}}$.

For all the cycles, t_{FR} was found to be either well within the pre-breakthrough period (cycles 2, 5 and 6) or to coincide with breakthrough (cycles 3 and 4). Recall that the first cycle started from a H_2-reduced catalyst and thus Eq. 7 would only apply to the following cycles. On this basis, the processes of steam reforming, carbonation and reduction of NiO to Ni would appear to have occurred alongside one another. It is noteworthy that when comparing the contributions of the two fuel consuming reactions (reduction of NiO via UC) and SR (steam reforming) to the total fuel conversion, the steam reforming was dominant across the cycles 2-6. This is illustrated in Table 3 by the % ratio 'R_{red}' of the estimated NiO reduction rate per cycle in pre-breakthrough to the maximum possible reduction rate for the same cycle via UC, defined by Eq. 8 below:

$$\left(R_{red} = 100 \times \frac{\dot{n}_{NiO \rightarrow Ni,PB}}{\dot{n}_{WCO,in} X_{WCO,SS} \left(2n + 0.5m - k\right)} \right) \quad \text{Eq. 8}$$

where this maximum reduction rate is reached in the absence of steam reforming. The results in Table 3 indicate that, since R_{red} remained between 10 and 20 % for all the relevant cycles (2-6), most of the fuel conversion would have resulted from steam reforming. This was shown to be also the case in the study without sorbent. A possible uncertainty about the % reduction state of the bed in the initial stages of the fuel feed may arise from the fact that there was an initial time t_0 between the start of the mixture feed and the first detection of H_2 by the online thermal conductivity analyser. One could interpret t_0 as representing two periods, a first non-reactive (long) period accounting for all the feeds to transport through the piping, reactor and analysers, and possibly, a shorter reactive second period where all or a significant amount of the WCO could have converted via solely the NiO reduction via the unmixed combustion (UC) reaction. Its CO_2 product would have been captured by the sorbent, and its co-product H_2O would have

condensed in the water trap, resulting in no dry gas products being detected, in this aspect making it indistinct from a non-reactive period. The 40 g of the catalyst, corresponding to 9.64×10^{-2} mol of Ni, would have fully reduced in only 63 s if a full conversion of the WCO had occurred via UC. In the absence of an accurate way of monitoring the onset of build up of water condensate, it was not possible to differentiate between non-reactive and potentially reactive periods 'pre-t_0' due to the presence of the sorbent. To circumvent this uncertainty, we use the outputs of the experiments carried out without the sorbent to assess whether an initial reactive 'reducing-only' period was likely to have occurred. In the absence of sorbent, if the reduction reaction UC had initially occurred on its own, CO_2 would have been detected in significant concentrations well before H_2. For instance, this was observed in a previous study using methane as the fuel (Dupont et al, 2008). A fuel conversion would then be derived from the rate of evolution of CO_2. In addition, the hydrogen elemental balance would also yield a significant negative steam conversion, as water would have been produced by UC, (rather than consumed by SR and WGS). Further, a peak in the NiO reduction rate would result from the elemental O balance. All of these were observed in Dupont et al (2008) when using methane as the fuel in chemical looping reforming conditions. However, it was clear from observing the outputs of the experiments with 40 g of catalyst without sorbent, that none of these manifestations had occurred with the present experiments with the WCO fuel. This is shown in Figs. 3a-b, which display the dry syngas mol fractions and the water conversion fraction for cycle 4 without sorbent, as a representative of typical 'no-sorbent' cycle behaviour. Figure 3a shows a CO_2 profile that started slightly earlier than the H_2 profile but not in significant amount, which then translated into a steam conversion fraction that exhibited a very small initial negative dip due to UC, immediately followed by a much more significant rise in positive values caused by SR and WGS (Fig. 3b).

Thus in the presence of the sorbent, a reducing-only initial period would most likely have been briefly present but with expected very small activity even if sorption enhanced by Carb, and the reduction of the NiO would have been gradual, occurring alongside the steam reforming and carbonation reactions. This then further reinforced the assumptions made earlier to derive Eq. 7 and the integration of the NiO reduction rate from time t_0 and not before. This finding is significant, as, had the reducing reaction occurred prior to the steam reforming/water gas shift reactions, the production of pure hydrogen would have been delayed. Upon up-scaling of the process, this would cause exaggerated intermittency in the production of H_2. The combination of the WCO fuel with the sorption enhanced chemical looping reforming process using this Ni-Al_2O_3 catalyst was therefore a beneficial one, as the Ni catalyst did not seem to require full reduction nor full fuel conversion prior to becoming active in hydrogen production by steam reforming and water gas shift.

3.2 *Process outputs during air feed*

During the air feed, four main reactions were susceptible to occur: the two carbon oxidation reactions (C-Ox and C-POx), the nickel oxidation reaction (Ni-Ox) and the calcination of the sorbent (Calc). Both C-Ox and Calc would have generated CO_2, while the three reactions C-Ox,C-POx and Ni-Ox consumed oxygen, therefore the carbon and oxygen elemental balances were not sufficient to determine the three unknown rates of Ni oxidation, carbon oxidation, and sorbent calcination. Thus a qualitative discussion is carried out in the following section. Figure 4(a) plots the rates of evolution of CO_2 and CO with time-on-stream during the air feed of the first cycle, juxtaposed with the mid-reactor and top-reactor temperatures curves. As soon as the temperatures exceeded the set temperature of 600 °C, the power to the reactor's heating coil was automatically cut-off, and this corresponded to a period of time of ca. 400 s. This period ended

with O_2 concentration in the products recovering from a low mol fraction to ca. 21% of the air feed (not shown). A period of flushing of the products from the previous feeds was observed for the initial 200 s, as was observed and discussed in the experiments carried out without the sorbent (Pimenidou et al, 2010). This was identified thanks to the matching profiles of CH_4 and H_2 (peaks not shown), which could only have formed during the WCO/steam/N_2 feed. Some CO and CO_2 also evolved during this flushing period. Between 300 and 500 s, CO_2 increased as a result of carbon oxidation, followed by a CO increase when the lack of oxygen hampered complete oxidation. We have shown in the study without sorbent and using the O elemental balance, that at this stage, Ni oxidation also occurred, and began its trend to dominate the consumption of oxygen. The exothermicity of these simultaneous oxidation reactions contributed to a rise in the reactor bed temperatures from 600 to above 800 °C (Fig. 4a).

It was expected that when the bed temperatures exceed 750 °C, de-carbonation would occur, but it is possible that larger solid temperature gradients deep in the bed material would allow for a more significant de-carbonation to take place. These solid temperature gradients would not have been accurately reflected by the thermocouple temperatures, which would have been closer to bulk gas reactor temperatures. This would explain how, when multiplying the peak rate of CO_2 evolution (4×10^{-4} mol/s) under air feed, by the assumed duration of the de-carbonation (the 300 s indicated in Fig. 4a by temperature exceeding 750 °C), only 29% of the CO_2 capacity of the sorbent was accounted for. In contrast, as seen previously in Table 2, the next carbonation cycle under fuel feed allowed for 46% of the capacity to be reached. This suggested a significantly longer de-carbonation period than that indicated by the duration for which thermocouple temperatures exceeded 750 °C, and would support higher solid temperatures at the seat of the

oxidation reactions able to better couple with the endothermic decarbonation (calcination) reaction.

Considering the WCO/steam/N_2 and air feeds as the two main reactive cycle conditions, and ignoring the potential reactivity of the N_2 purge, such as carbonaceous deposits playing a role in the reduction of NiO (Dupont et al, 2008), the advantages of the sorption enhanced chemical looping reforming process were demonstrated over a restricted number of cycles. These included production of high purity H_2, improved fuel and steam conversion, and autothermality for extended periods of time, as well as the ability to cope with partial fuel conversion without deleterious effects of carbon deposits, due to integration of the oxygen transfer catalyst and sorbent regeneration steps within the process. Thus on one hand, these features make the process very promising, and this, coupled with the fact that the chosen fuel, waste cooking oil, will remain in plentiful supply for the foreseeable future, would justify further research and development. On the other hand, the results revealed complex reaction mechanisms at work, where individual steps were difficult to isolate and quantify with the current set up and methods. For a better understanding of all the significant reactions in the process and of their interactions, fundamental studies with increased analytical capabilities in monitoring the extent of the OTM's redox states and sorbent's usage with time on stream appear necessary. In addition, although the process was shown to operate without obvious deterioration for six cycles, tests designed to establish the life expectancy of the OTM and sorbent in the conditions of sorption enhanced chemical looping reforming in packed bed configuration, and the extent to which their chemical reactivity influences the process would be desirable.

4. Conclusion

The chemical looping reforming of waste cooking vegetable oil on a Ni-Al_2O_3 catalyst in the presence of dolomite for in-situ CO_2 sorption has been shown to operate for six cycles at 600 °C at a steam to carbon ratio of 4 without obvious deterioration in fuel and steam conversion, H_2 purity and carbon products selectivity. Better fuel and steam conversions than in the absence of sorbent, carbonation efficiencies that stabilised around 56% of the ideal value for the following 5 cycles, and evidence of regeneration of both the catalyst and the sorbent under the two types of feeds were found.

Appendix: Nomenclature

α	Carbonation efficiency (%)
BT	Suffix relevant to the CO_2-breakthrough regime (carbonation with sorbent saturation)
Calc	Decarbonation (calcination) reaction ($CaCO_3 \rightarrow CaO+CO_2$)
Carb	Reaction of carbonation of the solid sorbent ($CaO+CO_2 \rightarrow CaCO_3$)
C-Ox	Complete carbon oxidation reaction ($C+O_2 \rightarrow CO_2$)
C-POx	Partial carbon oxidation reaction ($C+0.5O_2 \rightarrow CO$)
H_2 % pur	Hydrogen purity (%) calculated by $100\times(y_{H2}/(y_{H2}+y_{CO}+y_{CO2}+y_{CH4}))$
Ni-Ox	Nickel oxidation reaction ($Ni+0.5O_2 \rightarrow NiO$)
$\dot{n}$	Molar rate (mol s^{-1})
n, *m*, *k*	Elemental amounts of C, H and O in the fuel (mol)

OTM Oxygen transfer material

PB Suffix relevant to the pre-CO_2 breakthrough regime (during carbonation)

Sel Selectivity to a specific product (%)

SS Suffix relevant to CO_2-steady state or post-CO_2 breakthrough conditions.

SR Steam reforming reaction ($C_nH_mO_k$ reacting with steam producing CO and H_2)

t Characteristic time (s)

Tmid Mid reactor bed temperature (°C)

UC Unmixed combustion reaction (reduction of NiO by $C_nH_mO_k$, producing Ni, CO_2, and H_2O)

WCO Waste cooking vegetable oil

WGS Water gas shift reaction ($CO+H_2O \leftrightarrow CO_2+H_2$)

X Fractional conversion

y Gas mol fraction

Acknowledgments

Our thanks to the Engineering and Physical Research Science Council (EPSRC) for grant EP/D078199/1, to Johnson Matthey for catalysts and WBB Minerals for the dolomite from the Warmsworth quarry.

References

Devi, L., Ptasinski, K. J., Janssen, F. J. J. G, van Paasen, S. V. B., Bergman, P. C. A., Kiel, J. H. A, 2005. Catalytic decomposition of biomass tars: use of dolomite and untreated olivine. Renew. Energ., 30, 565- 587.

Dupont, V., Ross, A. B., Hanley, I., Twigg, M. V., 2007. Unmixed Steam Reforming of Methane and Sunflower Oil: A Single-Reactor Process for H_2-rich Gas. Int. J. Hydrogen Energ., 32, 67-79

Dupont, V., A. B. Ross, E. Knight, I. Hanley, M. V. Twigg, 2008. Production of hydrogen by unmixed steam reforming of methane. Chem. Eng. Sci., 63, 2966-2979.

Eder, K, and Brandsch, C., 2002. The effect of fatty acid composition of rapeseed oil on plasma lipids and oxidative stability of low-density lipoproteins in cholesterol-fed hamsters. Eur. J. Lipid Sci. Technol., 104, 3-13.

Harrison, D.P., 2008. Sorption-enhanced hydrogen production: A review. Ind. Eng. Chem. Res. 47, 6486-6501.

Kee, R.J., Miller, J.A., Jefferson, T.H., 1980. CHEMKIN: a general purpose problem-independent, transportable, FORTRAN Chemical Kinetics Code Package. Sandia National Laboratories. Report SAND80-8003.

Lutz, A.E.; Rupley, F.M.; Kee, R.J. 1999, *EQUIL: a Program for Computing Chemical Equilibria. CHEMKIN Collection, Release 3.5*; Reaction Design, Inc: SanDiego, pp 2-20.

Myren, C., Hoernell, C., Bjornbom, E., Sjostrom, K., 2002. Catalytic tar decomposition of biomass pyrolysis gas with a combination of dolomite and silica. Biomass Bioenerg. 23, 217-227.

Pimenidou, P., Rickett, G.L., Dupont, V. 2009. In-situ CO_2 capture for unmixed steam reforming. Oral presentation at WCCE8 (8^{th} World Congress of Chemical Engineering). August 23-27 2009, Montreal, Canada.

Pimenidou, P., Rickett, G.L., Dupont, V., and Twigg, M. V., 2010. Chemical looping reforming of waste cooking oil in packed bed reactor. Accepted in Bioresource Technol. BITE-D-10-00048, in press.

Simell, P. A., son Bredenberg, J.-B., 1990. Catalytic purification of tarry fuel gas. Fuel, 69, 1219-1225

Table 1 Process outputs at steady state (post-CO_2 breakthrough) for 6 cycles without (left) and with (right) the CO_2 sorbent present (40 g of catalyst, S:C ratio of 4, set reactor temperature of 600 °C).

	Without sorbent							With 40 g of calcined dolomite						
C	*X WCO*	*X* H_2O	*Sel CO*	*Sel* CO_2	*Sel* CH_4	H_2 % pur	T mid	*X WCO*	*X* H_2O	*Sel CO*	*Sel* CO_2	*Sel* CH_4	H_2 % pur	T mid
1	0.19	0.07	12	86	2	70.5	579	0.46	0.19	4	81	15	69.7	584
2	0.21	0.07	16	80	4	68.9	585	0.30	0.11	10	89	1	71.3	597
3	0.20	0.06	20	74	5	68.5	585	0.31	0.10	10	89	1	70.5	604
4	0.14	0.06	23	70	7	67.3	589	0.32	0.12	11	87	2	70.1	604
5	0.22	0.05	16	68	16	64.8	587	0.23	0.08	11	86	3	70.6	604
6	0.20	0.07	23	69	7	68.8	591	0.27	0.11	16	78	6	72.3	601
av	0.19	0.06	18	75	7	68.1	586	0.31	0.12	10	85	5	70.7	599

Table 2 Durations of CO_2 pre-breakthrough and breakthrough periods, pre-breakthrough rate of carbonation, carbonation efficiencies prior to- and during CO_2 breakthrough, and total carbonation efficiency for each cycle during the chemical looping reforming of WCO at S:C of 4 with sorbent and the set reactor temperature of 600 °C.

Cycle	t_0	$t_{BT} - t_0$ (s)	$t_{SS} - t_{BT}$ (s)	$\dot{n}_{CO_2,carb,PB}$ (mol s^{-1})	α_{PB} (%)	α_{BT} (%)	α (%)
1	230	1270	990	2.42×10^{-4}	73.7	27.3	101
2	400	750	550	1.59×10^{-4}	34.2	12.0	46.2
3	2290	1105	555	1.61×10^{-4}	42.6	12.6	55.2
4	1700	1000	725	1.70×10^{-4}	40.7	20.2	60.9
5	1500	1025	890	1.22×10^{-4}	17.3	35.9	53.2
6	1800	1480	545	1.42×10^{-4}	50.3	13.8	64.1

Table 3 Estimate of NiO reduction rate in pre-CO_2 breakthrough conditions and % ratio of NiO reduction rate to maximum reduction rate achievable by fuel conversion $\left(R_{red} = 100 \times \frac{\dot{n}_{NiO \rightarrow Ni,PB}}{\dot{n}_{WCO,in} X_{WCO,SS} \left(2n + 0.5m - k\right)} \right)$ for cycles 2-6 and same conditions as Table 2.

Cycle	$\dot{n}_{NiO \rightarrow Ni,PB}$ (mol s^{-1})	% R_{red}
2	0.66×10^{-4}	14.5
3	0.84×10^{-4}	18.0
4	1.01×10^{-4}	20.5
5	0.61×10^{-4}	17.2
6	0.41×10^{-4}	10.0

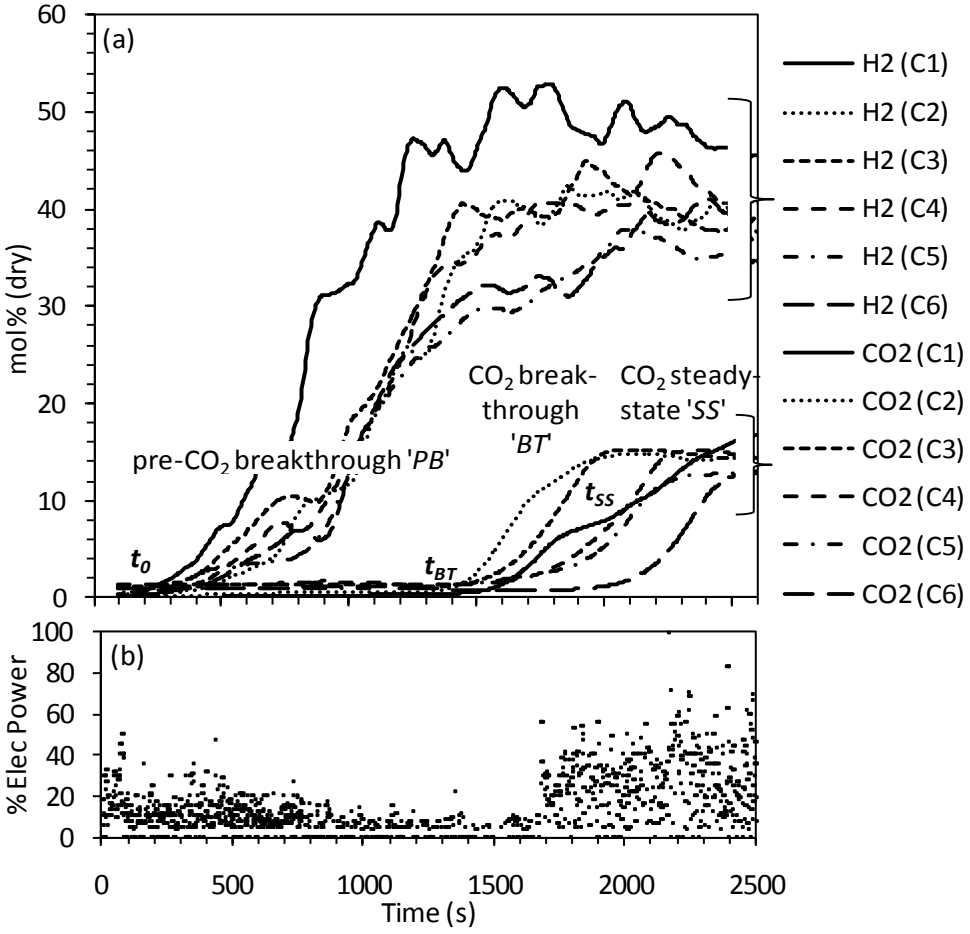

Fig. 1(a) Dry mol % of H_2 (upper curves group) and CO_2 (lower curves group) for each cycle (C1-6) measured online every 5 s during the WCO/steam/N_2 feed with 40 g of catalyst and 40 g of calcined dolomite, using a S:C of 4 at a set reactor temperature of 600 °C. (b) Electrical power input to the reactor for the first cycle (% of maximum).

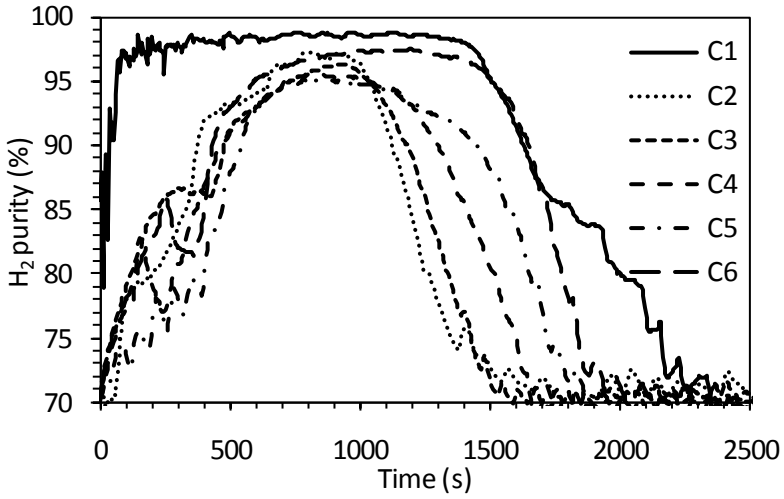

Fig. 2 H_2 % purity for cycles C1-6 in same experimental conditions as Fig. 1. End values near 70% after high plateau (post CO_2-breakthrough) correspond to tabulated values in Table 1.

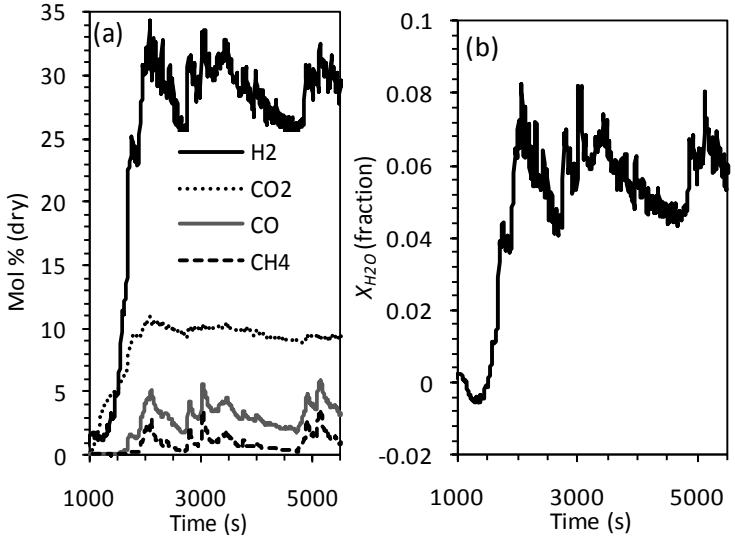

Fig. 3 (a) Dry syngas mol fractions and (b) estimated water conversion fraction for cycle 4 without sorbent, 40 g catalyst, S:C=4, T_{set}=600 °C, same flows as in Fig. 1.

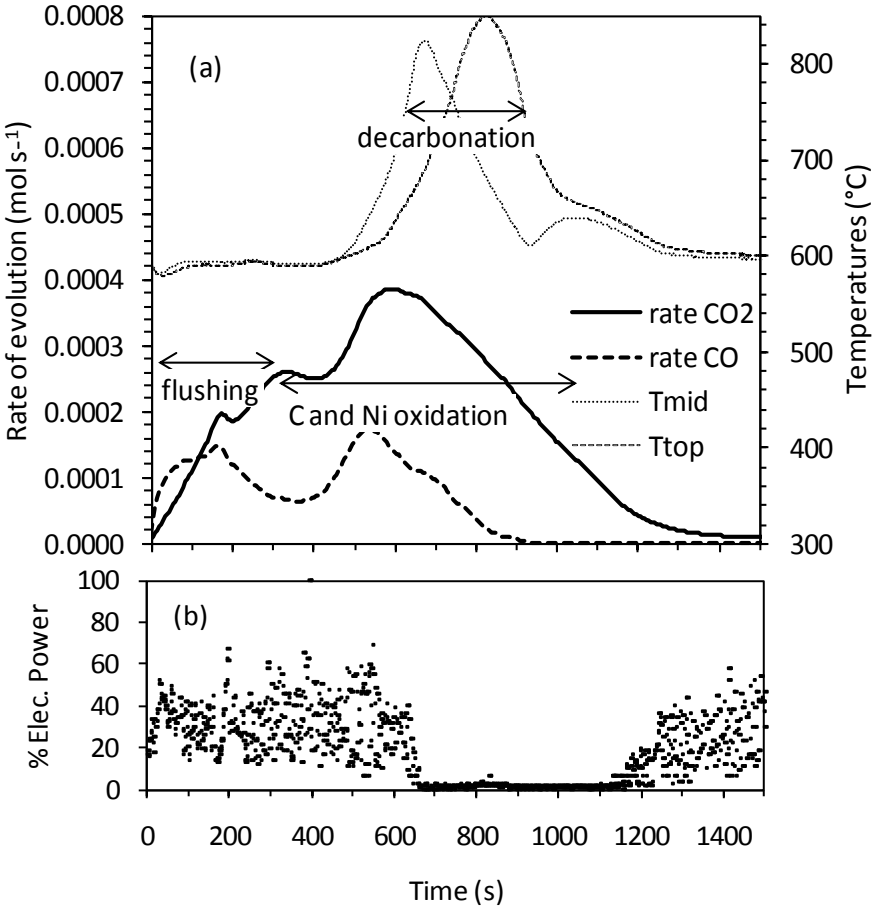

Fig. 4 (a) Rates of CO_2 and CO evolution for the air feed of the first cycle with sorbent (bottom curves) and mid- and top-reactor temperature-time curves (top). (b) Percent electrical power input to the heater during air feed of first cycle.